

# **FUEL SLOSH AS AN ENHANCED FLAMMABILITY CONCERN FOR AIRCRAFT**

**Peter J Disimile**

UC-FEST, Dept of Aerospace Engineering  
University of Cincinnati, Ohio 45221

[Peter.Disimile@uc.edu](mailto:Peter.Disimile@uc.edu)

(513) 556-3355

**John Pyles & Norman Toy**

Engineering & Scientific Innovations, Inc.  
Blue Ash, Ohio 45241

[Dr.Toy@esi-solutionsinc.com](mailto:Dr.Toy@esi-solutionsinc.com)

(513) 277-0516

## **Abstract**

Past research suggests that droplets and liquid/air mixing may enhance the flammability limits of the fuel within a tank. However, the liquid dynamics have yet to be characterized under even the simplest of aircraft maneuvers. To improve our understanding of this hazard an experimental investigation of liquid dynamics of water in a rectangular tank experiencing aircraft dynamics was undertaken using a state-of-the art motion simulator to examine low frequency, low amplitude roll oscillations. A high-speed imaging system was used to capture the event and two major flow phenomena were captured; a hydraulic jump and wave interactions. The former poses a significant vulnerability hazard due to droplet separation and enhanced liquid/air mixing and may create localized regions of flammable fuel/oxygen mixtures in an otherwise inerted tank, whereas the latter produces droplet separation through interaction and may behave as secondary ignition sources that are self-sustaining. An investigation of the physical characteristics of the hydraulic jump formation as well as the location of wave interactions was carried out for consideration for improved aircraft vulnerability. This research is currently the initial phase of a three-phase project to understand ignition vulnerabilities in a dynamic fuel tank environment.

## Introduction

The 1996 TWA flight 800 incident off the New York coast has renewed interest in fuel tank fire prevention under typical aircraft dynamics. The National Transportation Safety Board (NTSB) ruled that this incident occurred as a result of “explosion of the center wing fuel tank (CWT), resulting from ignition of the flammable fuel-air mixture in the tank<sup>1</sup>.” As a result, the aviation community has called for improved safety measures to prevent accidental or intentional ignition of aircraft fuel tanks, including revising the safe lower oxygen concentration limit for inerting fuel tanks.

When liquid in a tank experiences dynamic motion, a variety of wave interactions and liquid phenomena can exist. The motion of the bulk liquid is dependent on the depth of the liquid within the tank and is characterized by a resonance frequency based on the liquid depth. From an aircraft controls standpoint, liquid dynamics plays a large role in aircraft design. Liquid motion in a variety of tank geometries has been studied theoretically to help predict structural moments due to liquid sloshing on aircraft<sup>2</sup>. For the purposes of this research, only rectangular tank geometries will be discussed. Both theoretical<sup>3-5</sup> and experimental<sup>6-7</sup> studies have been undertaken for the case of rectangular tanks of length  $B$ , width  $L$ , and liquid depth  $h_0$  above the floor of the tank, experiencing two-dimensional oscillation about the  $B/2$  axis. It has been shown in the literature that the resonance frequency for a liquid depth  $h_0$  can be expressed as:

$$f_n = \frac{1}{2\pi} \left[ \frac{g\pi(n+1)}{B} \tanh\left(\frac{(n+1)\pi h_0}{B}\right) \right]^{1/2} \quad n = 0, 1, 2, \dots, \infty \quad 1$$

When the tank is oscillated at the resonance frequency based on the liquid depth, a hydraulic jump is observed traversing the tank<sup>7</sup>. Hydraulic jumps are characterized by a rapid change in depth with a turbulent, air/liquid mixing region between the two depths. They occur when a wave caused by a perturbation exceeds the wave celerity, or the maximum velocity a surface wave can travel for a given liquid depth. For open channel flows, flows traveling above the wave celerity are known as supercritical and below the wave celerity are called subcritical. As a result, the direction in which surface waves travel is affected by the flow condition. In the supercritical condition, perturbations created on the surface of the liquid cause waves to travel with the direction of the flow. On the other hand, surface waves can travel upstream and downstream in the subcritical condition<sup>8</sup>.

The fluid dynamics of liquid inside a dynamic fuel tank environment is of special interest to ignition vulnerability research and has brought into question current flammability limits and safe maximum oxygen concentration stated by the Federal Aviation Administration (FAA). Currently, some fuel tanks are inerted through the injection of nitrogen, reducing the oxygen concentration. Also, the current safe operating temperatures for a fuel tank are based on static and homogeneous testing<sup>2-5</sup>. However, the complexity of the liquid/air interactions in a dynamic fuel tank can pose various vulnerability threats not observed in static testing to the ullage, the space above the liquid layer. Spray and foam formations can enhance fuel/air mixing, which, in turn, can create localized, stoichiometric fuel/oxygen concentrations in an otherwise inerted ullage. Although these phenomena may be present in an aircraft fuel tank during a flight, there

have been few studies on the characterization of the liquid/air interactions in the dynamic aircraft environment.

Enhanced flammability research in dynamic fuel tank environments has not been extensively studied despite indications that discrepancies exist between static and dynamic test results. Nestor<sup>13</sup> performed one of the first investigations into the flammability hazards of a fuel sloshing in a tank while studying the dynamic conditions within a fuel tank. Similar research was conducted by Ott<sup>14-15</sup> several years later. Both researchers tested the static and dynamic flammability limits of commercial Jet A<sup>13</sup> or military JP-8 fuel<sup>14-15</sup>. Liquid fuel temperatures between 34 °C and 83 °C produce a sufficient amount of fuel vapors to sustain an ignition at ambient pressure and oxygen concentration (21% by volume). Both researchers noted that dynamic conditions increased the flammability envelope significantly at the lower flammability limit (from a fuel temperature of 34 °C to 10 °C at standard atmospheric pressure). Research by Ott<sup>15</sup> suggested little effect on the lower oxygen concentration requirement. The researchers believed that droplet and mist formation caused by the motion of the liquid in the tank play an important role in the increased probability of ignition at lower fuel temperatures. However, characterization of these events was not examined.

This initial research will examine the liquid dynamics within a rectangular tank experiencing near resonance oscillations based on the liquid depth of water. Areas where sprays form due to hydraulic jumps or wave interactions will be located. Understanding these two types of events from an enhanced flammability perspective can lead to improved comprehension of dynamic fuel tank flammability as well as improved mitigation methods of dynamic liquid phenomena. Furthermore, this initial phase research will act as a visual guide for fuel tank ignition tests conducted under dynamic conditions in the final phase of this project.

### **Experimental Setup**

A testing facility at Wright-Patterson Air Force Base was utilized for an investigation on the effect of low frequency, small amplitude roll oscillations on the liquid dynamics in a rectangular tank. The test facility consisted of a state-of-the-art motion simulator and a rectangular tank with three transparent sides.

To replicate generic roll aircraft dynamics, a hydraulically activated Sarnicola Hexad AIES Six-Degree-of-Freedom motion simulator was employed. This simulator has base dimensions of 3.28 m (129”) x 2.03 m (80”) at a rest height of 1.73 m (68”), and it is capable of carrying an 11,364 kg (25,000 lb) payload. This motion simulator has 6 degrees of freedom provided by six hydraulic cylinders or actuators and is controlled through proprietary computer software called HexTest. The hydraulic cylinders are arranged in a hexapod configuration that allows for maximum rotational excursions, Figure 1.

A generic clear tank of simple design provided optical access to three spatial planes through the top, side, and front of the tank by means of 25.4 mm (1”) thick walls of Lexan with the other walls fabricated from 6.35 mm (0.25”) thick steel. An interior steel frame was constructed to provide additional reinforcement for the Lexan sides. The clear tank frame supports a tank with overall internal dimensions of 1.9 m (73”) x 1.2 m (48”) x 0.94 m (37”), yielding a maximum

capacity of  $2.1 \text{ m}^3$  (563 gal), and will provide a larger scale study than any previous experiments discussed in the previous section. Lexan walls with a thickness of 12.7 mm (0.5") were added on the outside of the open sides of the tank shell to provide optical access in each spatial plane. The steel sides of the frame provided the internal tank walls for the remaining sides. The generic tank was positioned inside of the steel shell constructed of 6.35 mm (0.25") thick steel tubing and placed on the motion simulator. Steel tubing located on the top and two steel bars along the clear side of the tank provide additional support for the Lexan walls.

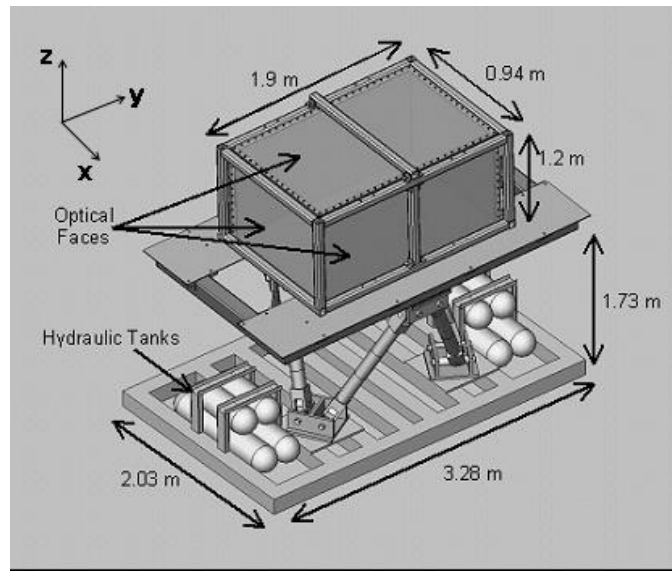


**Figure 1: Overall Simulator and Slosh Tank Setup**

A high-speed digital Nanosense XS-3 CMOS camera from IDT with a resolution of  $1280 \times 1024$  pixels was utilized to capture the liquid dynamics within the tank. The camera was positioned on a tripod at a height of 1.93 m (76") at a distance of 2.24 m (88") from the front wall of the tank fixture. A 20 mm Nikon lens was attached to the camera and captured the full field of view of the test apparatus. The digital imaging system acquired video at 75 Hz for a total of 15 seconds at the start of the oscillation. All images were stored in the onboard camera memory and then transferred to the computer via the USB 2.0 connection upon completion of each test for analysis. The complete test setup is shown in Figure 2.

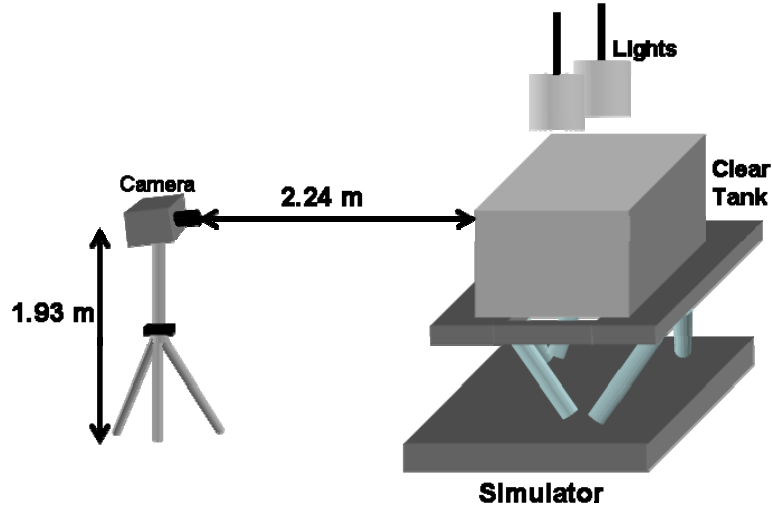


**Figure 2: Test Setup**

**Testing Conditions**

Three liquid depths were selected for the examination of liquid separation phenomena in oscillating containers and are shown in Table 1 along with the resonance frequency of the depth.

**Table 1: Liquid depths and fundamental resonance frequency**

| Liquid Depth (m) | Resonance Frequency, $f_0$ (Hz) |
|------------------|---------------------------------|
| 0.265            | 0.42                            |
| 0.371            | 0.50                            |
| 0.530            | 0.60                            |

These depths were selected based on their low resonance frequencies and necessary volume to produce a vulnerable amount of fuel vapor for ignition. Furthermore, these depths can produce a large amount of spray from the wave impacting an end wall. Water was used in place of jet fuel due to safety concerns.

The tank was oscillated at frequencies ranging between 0.20 – 0.50 Hz and oscillation amplitudes of  $2.42^0$ ,  $3.50^0$ , and  $4.71^0$  according to the expression in eqn (2) for each liquid depth. These oscillation amplitudes represent 10%, 15%, and 20% of the maximum roll amplitude of the simulator. A slight offset,  $A$ , had to be introduced due to a bias in the motion simulator when the centre of gravity (CG) is shifted from its manufactured position. The asymmetry of the tank walls caused this shift in the CG.

$$\theta(t) = \theta_0 \sin(\omega t - \phi) + A \tag{2}$$

## Data Analysis

All post processing analysis was performed in the X-Vision software from IDT. The software was utilized to time stamp and measure the spatial locations of the wave interactions and hydraulic jump formations. Each event was enlarged and its significant pixel locations noted. Also, the pixel locations of the bottom corners of the tank were recorded to provide insight into the angle of the tank as well as relative jump location with respect to the bottom and sides of the tank. A calibrated scale was positioned on the tank to determine a calibration coefficient. The calibration coefficient was then used to calculate the separation phenomena spatially within the tank.

## Results

Each digital video was visually analyzed for spray and droplet formation due to wave interactions and hydraulic jump formation. The location of each of these events was measured via the camera software. It was visually observed that there were three modes of droplet separation:

- Wave impacting the tank end walls
- Hydraulic jump formations
- Wave-wave interactions

For the purposes of this research, only the latter two will be discussed. A hydraulic jump formation for a water depth of 0.265 m is shown below in Figure 3 and droplet separation due to wave interaction in a 0.371 m depth of water is shown in Figure 4.

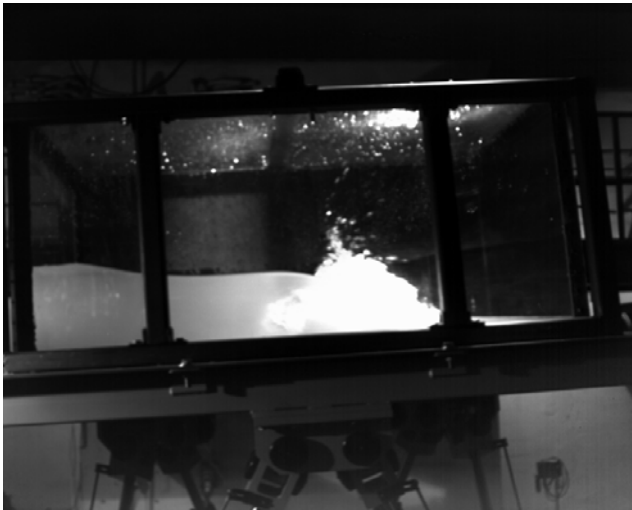


**Figure 3: Hydraulic Jump**



**Figure 4: Wave Interaction**

## Hydraulic Jump Formation

Hydraulic jumps were visually observed in liquid depths of 0.265 m and 0.371 m for the range of frequencies and amplitudes discussed in the previous section. The tank was oscillated at driven frequencies near the fundamental resonance frequency ( $f_0$ ) based on the liquid depth. This was sufficient in inducing the formation of hydraulic jumps and it was observed traveling back and forth along the length of the tank. The incline angle of the tank was calculated as a function of time and is represented by the solid or dashed lines in Figure 5. The time that a hydraulic jump forms and the angle of the tank at this time were measured via the digital video and are represented by the data points in the graphs. Right traveling and left traveling hydraulic jumps form at the same frequency as the driven tank oscillation but at different tank angles.

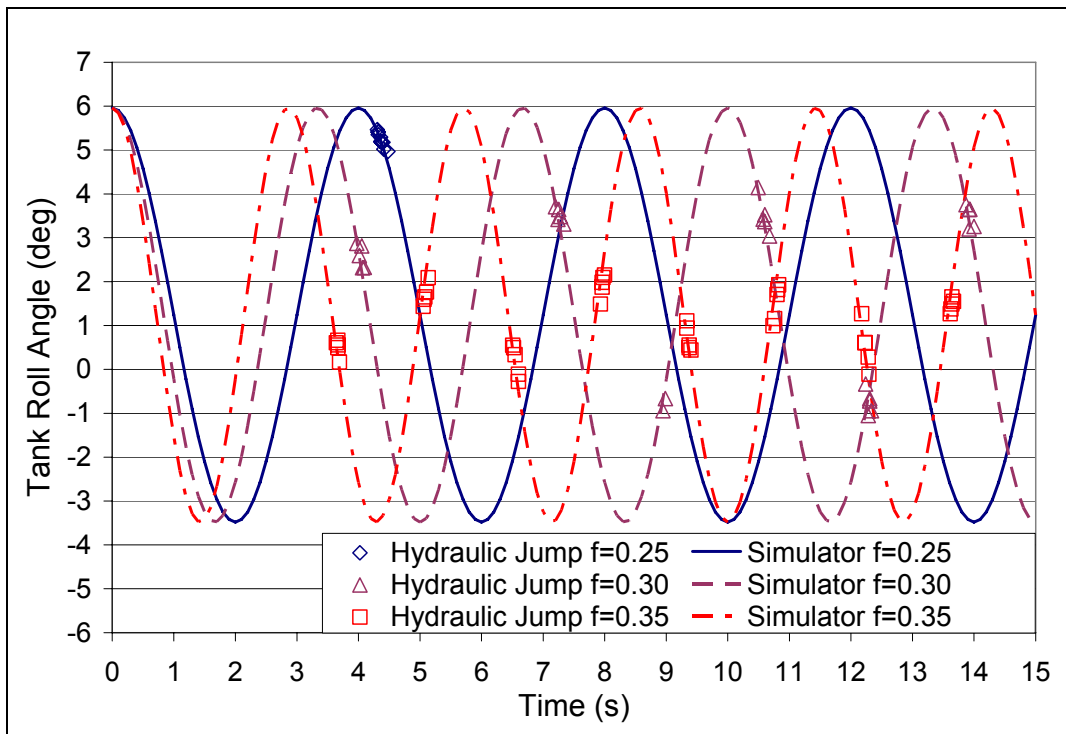


**Figure 5: Hydraulic Jump Formation**

The oscillation of the hydraulic jump formation appears out of phase with the oscillation of the tank. It is suggested by Verhagen et al<sup>6</sup> that the phase of the hydraulic jump formation is related to the formation location of the jump. For example, if the jump is  $90^\circ$  out of phase with the tank oscillation, the jump forms at the center of the tank. As the phase angle decreases, the location of the jump formation tends to move towards the end wall. The absolute phase difference between the tank oscillation and hydraulic jump formation was calculated for each data point. The absolute phase difference was determined by measuring the time difference,  $t_{diff}$ , between the peak of the tank oscillation and adjacent hydraulic jump formation. Multiplying this value by the angular frequency of the tank oscillation yielded the phase difference between the jump formation and tank oscillation; equation 3.

$$\phi_{diff} = (2\pi f_0) t_{diff}$$

The average absolute phase difference for the three amplitudes was calculated and averaged for each oscillation condition and the results of this determination are presented in Figure 6. The data is plotted as the ratio of the driven frequency,  $f$ , to the resonances frequency of the depth,  $f_0$ , shown in Table 1. The data set was plotted independently of the oscillation amplitude and was fitted with a linear interpolation, yielding a correlation coefficient of 0.5635 for the data set. This fit is suggested by Verhagen et al<sup>6</sup> using shallow water wave theory. It can be seen from Figure 6 that as the frequency of the oscillation approaches the resonant frequency based on the liquid depth, the hydraulic jump formation tends to the center of the tank, or 90° out of phase with the driven oscillation.

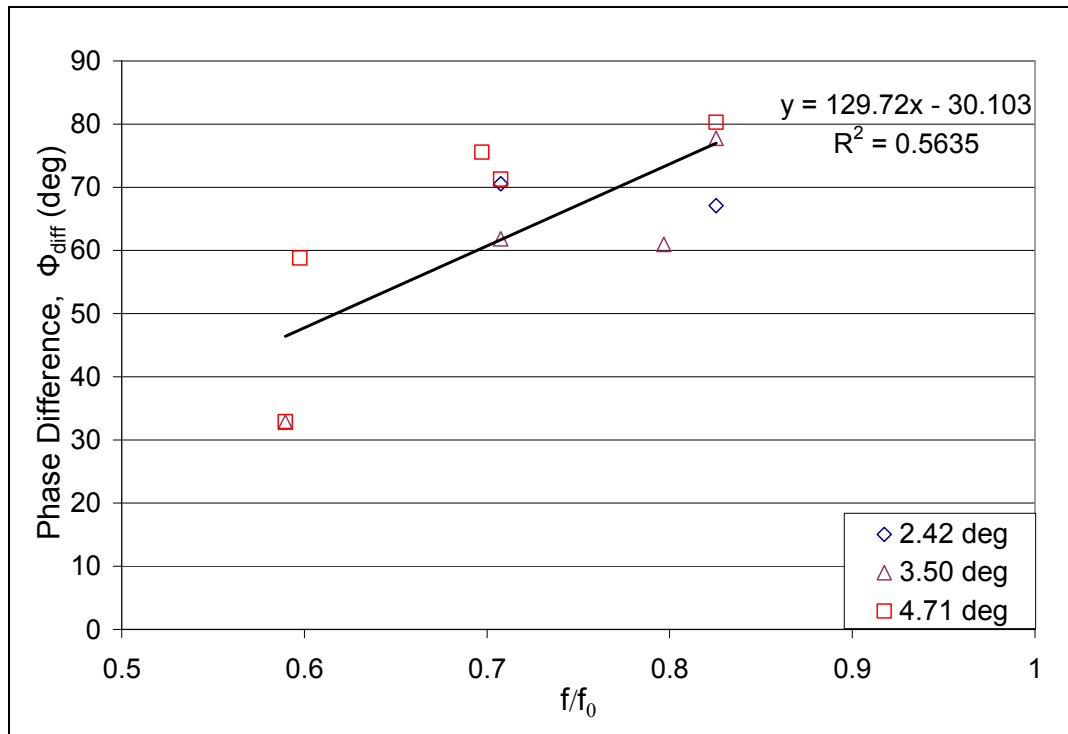


**Figure 6: Hydraulic Jump Phase Difference**

### Wave Interactions in a 0.265 m Liquid Depth (0.473 m<sup>3</sup> Volume)

The second phenomenon that was investigated in this research was the formation of droplets from the interaction of waves. The height at which these droplets were ejected from the liquid surface and the location along the length of the tank was measured. In the proceeding figures, the center of the tank is designated as  $x = 0$  and the y-axis represents the height at which droplets are observed. The shaded region on each of the figures represents the initial rest depth of the liquid.

For a liquid depth of 0.265 m (0.473 m<sup>3</sup> volume), droplet separation occurred at the following oscillation amplitudes and a roll frequency of 0.30 Hz for the 10% amplitude condition and 0.25 Hz for the 15% and 20% amplitude condition, Figure 7. Lower frequencies were tested but are not presented in the current research because droplet separation did not occur at these lower frequencies. For this liquid depth, a majority of the separation points occurred at or above the rest depth of the liquid and near the walls of the tank. The increase in amplitude from 10% to 20% appeared to coincide with an approximate 0.10 m increase in the separation height in the  $x > 0$  region of the tank. In the  $x < 0$  region of the tank, the same amplitude increase caused a 0.05 m decrease in separation height. Furthermore, the 20% amplitude and 0.25 Hz condition produced separation closest to the end walls of the tank. Increased amplitude from 10% to 20% caused the wave separation to occur approximately 0.2 m closer to the end walls of the tank.

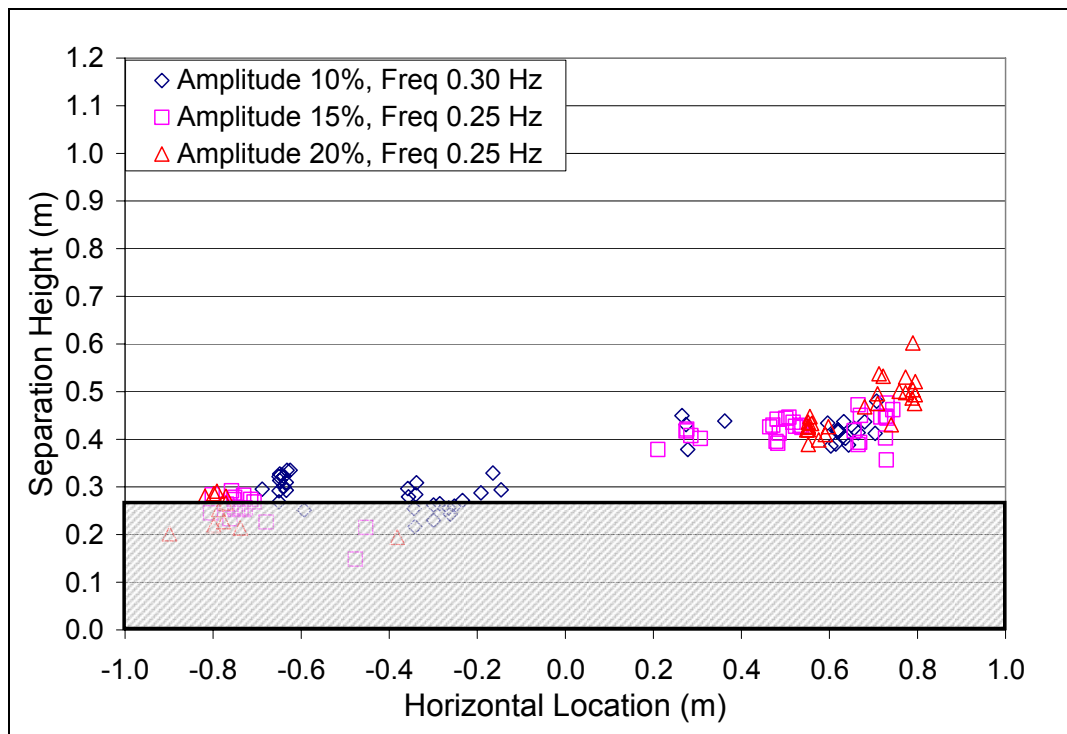


**Figure 7: Wave separation height at various tank locations for 0.265 m depth**

### Wave Interactions in a 0.371 m Liquid Depth (0.662 m<sup>3</sup> Volume)

For a liquid depth of 0.371 m, a large number of separation events were observed, Figure 8. Droplet separation occurred for frequencies as low as 0.30 Hz at 20% amplitude to as high as 0.40 Hz at 10% amplitude. At 10% oscillation amplitude and 0.35 Hz frequency, the wave separation points appear to be symmetric about the center of the tank ( $x = 0$ ) and occur at  $\pm 0.45$  m from the tank center. When the frequency was changed to 0.40 Hz for the same oscillation amplitude, the separation points occurred near the center of the tank and were more prevalent. In the 15% oscillation amplitude configurations, similar trends were noted. The 0.35 Hz oscillation frequency test condition produced droplet separation in approximately the same regions as the 10% amplitude condition for the same frequency. Also, some separation was noted near the center of the tank. For the 0.40 Hz oscillation frequency, the separation occurred near the center of the tank; however, it was at a slightly lower separation height than the 10% oscillation amplitude condition for the same frequency. It should also be noted that hydraulic jumps occurred for the test condition as well. Separation due to wave interaction occurred for the test condition of 20% oscillation amplitude at a frequency of 0.30 Hz. The horizontal separation points in this condition also appear to be symmetric about the center of the tank at a location of  $\pm 0.65$  m and  $\pm 0.15$  m from the center.

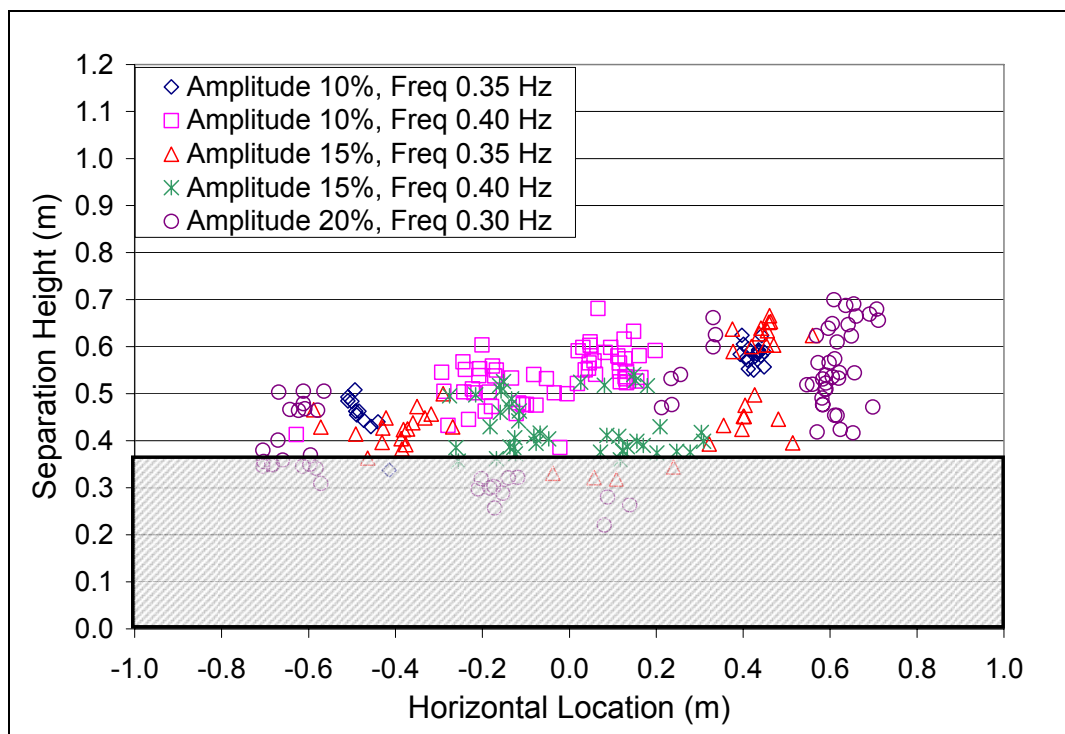


**Figure 8: Wave separation height at various tank locations for 0.371 m depth**



## Summary

It has been shown that even under the slightest of dynamic conditions; waves can form and interact with each other or with the end walls to produce droplets and spray. Past research suggests this spray can act as secondary ignition sources and can be self sustaining. As a result, this can enhance the flammability limits of a tank. This research utilizing water is an initial examination of the complex liquid dynamics that occur within a fuel tank. Distinct regions of separation and hydraulic jump formation are noted. Hydraulic jumps tended to form near the center of the tank as the tank oscillation frequency approached the resonance frequency based on the liquid depth. At the lower frequencies tested in the current research, the observed phenomenon that produced droplet separation was wave-wave interactions. Frequencies that produced the wave separation were found to be below the frequencies that produced hydraulic jumps. Furthermore, hydraulic jumps were not observed in tests that contained wave-wave interactions. Wave-wave interaction separation events were concentrated near the end walls of the tank for the 0.265 m and 0.530m depths and near the center for the 0.371 m depth. The irregularity of the separation heights observed in these tests suggests that the bias due to the asymmetry of the tank influences the results. This first phase of the research can be used to provide visual insight to the liquid conditions within an explosion proof tank containing flammable aviation fuel oscillated at the sloshing test conditions.

## References

- [1] "Accident Report: In-Flight Breakup Over the Atlantic Ocean Trans World Airlines Flight 800 Boeing 747-131, N93119, near East Moriches, New York, July 17, 1996," National Transportation Safety Board, NTSB/AAR-00/03, August 23, 2000.
- [2] Abramson, H. N. (ed.), "The Dynamic Behavior of Liquids in Moving Containers," NASA, NASA SP-106, Washington D. C., 1966.
- [3] Graham, E. W. and Rodriguez, A. M., "The Characteristics of Fuel Motion Which Affect Airplane Dynamics," *Journal of Applied Mechanics*, Vol. 123, No. 9, September 1952, pp. 381-388.
- [4] Fontenot, L. L., "Dynamic Stability of Space Vehicles: Volume VII – The Dynamics of Liquids in Fixed and Moving Containers," NASA, NASA CR-941, Washington D. C., March 1968.
- [5] Lee, T., Zhou, Z, and Cao, Y, "Numerical Simulations of Hydraulic Jumps in Water Sloshing and Water Impacting," *Journal of Fluids Engineering*, Vol. 124, March 2002, pp. 215-226.
- [6] Verhagen, J. H. G., and van Wijngaarden, L., "Non-Linear Oscillations of Fluid in a Container," *Journal of Fluid Mechanics*, Vol. 22, part 4, 1965 pp. 737-751.
- [7] Armenio, V., La Rocca, M., "On the Analysis of Sloshing of Water in Rectangular Containers: Numerical Study and Experimental Validation," *Ocean Engineering*, Vol. 23, No. 8, 1996, pp. 705-739.
- [8] Chaudhry, M. H., *Open Channel Flow*, Prentice Hall, Englewood Cliffs, N. J., 1993.
- [9] Kuchta, J. M., "Oxygen Dilution Requirements for Inerting Aircraft Fuel Tanks," *Second Conference on Fuel System Fire Safety*, Bureau of Mines Safety Research Center, Washington, D. C., May 1970, pp. 85-115.

- [10] Stewart, P. and Starkman, E., "Inerting Conditions for Aircraft Fuel Tanks," Wright Air Development Center, WADC Tech Report 55-418, Wright-Patterson Air Force Base, OH, September 1955.
- [11] Zinn, S., "Inerted Fuel Tank Oxygen Concentration Requirements," Federal Aviation Administration, FAA-RD-71-42, Atlantic City, NJ, August 1971.
- [12] Summer, S. M., "Limiting Oxygen Concentration Required to Inert Jet Fuel Vapors Existing at Reduced Fuel Tank Pressures," Federal Aviation Administration, DOT/FAA/ARTN-02/79, Washington D. C., August 2003.
- [13] Nestor, L. J., "Investigation of Turbine Fuel Flammability within Aircraft Fuel Tanks," Naval Air Propulsion Test Center, Aeronautical Engine Department, DS-67-7, Philadelphia, Pennsylvania, July 1967.
- [14] Ott, E. E., "Effects of Fuel Slosh and Vibration on the Flammability Hazards of Hydrocarbon Turbine Fuels Within Aircraft Fuel Tanks," Air Force Aero Propulsion Laboratory, AFAPL-TR-70-65, Wright-Patterson Air Force Base, Ohio, November 1970.
- [15] Ott, E. E. and Lillie, E., "Influence of Fuel Slosh Upon the Effectiveness of Nitrogen Inerting for Aircraft Fuel Tanks," Aero Propulsion Laboratory, II Preliminary Report, Wright Patterson Air Force Base, 1970.